Sensitivity of Doping States in the Copper Oxides to Electron-Lattice Coupling

K. Yonemitsu and A. R. Bishop
Theoretical Division, Los Alamos National Laboratory, Los Alamos, New Mexico 87545

J. Lorenzana
International School for Advanced Studies, Strada Costiera 11, 34014 Trieste, Italy
(Received 10 December 1991)

Doping states in a two-dimensional three-band Peierls-Hubbard model are investigated with inhomogeneous Hartree-Fock and random phase approximations. They are sensitive to small changes of electron-lattice and electron-electron interactions. For parameters relevant to the insulating copper oxides a small ferromagnetic polaron is found. Moderate intersite electron-lattice coupling triggers a nonlinear feedback mechanism resulting in a rapid crossover from a Zhang-Rice regime to a covalent molecular singlet state in which the local magnetic moment is quenched and local lattice distortion is large. Various states are characterized by distinct optical and infrared absorption spectra.

PACS numbers: 74.70.Vy, 71.38.+i, 75.30.Fv, 78.30.Er

Considerable modeling of high-temperature superconductors has focused on the identification of hole doping states (spin bags, polarons, excitons) defined with respect to insulating stoichiometric antiferromagnetic (AF) two-dimensional (2D) Cu-O ground states [1–3]. Here, we demonstrate that the nature of doping states and their interactions can be extremely sensitive to effects going beyond a pure 2D, one-band Hubbard model. In particular we find, within a 2D, three-band extended Peierls-Hubbard Hamiltonian, that a moderate intersite electron-lattice coupling triggers a rapid crossover from a small polaron with a well formed moment on Cu to a local collapse of the Cu magnetic moment and strong local lattice distortion in the strong AF background [see Fig. 1(a)]. This can be viewed as a transition from a Zhang-Rice singlet [4] to a covalent molecular state. For weak electron-lattice coupling the doping state is very sensitive to the on-site Cu Coulomb repulsion (U_d). By slightly increasing U_d from the value inferred from a local density approximation (LDA) calculation [5], we find a transition from the above-mentioned small polaron to an intermediate-size ferromagnetic polaron with spin densities perpendicular to the AF background. For sufficiently strong electron-lattice coupling the ground state changes completely to a nonmagnetic bond-order or charge-density-wave state. Large nearest-neighbor Cu-O Coulomb repulsion drives phase separation [6]. The various doping states produce distinct infrared and optical absorption spectra, relevant to chemical-doping [7] and photodoping [8] experiments.

We have used a Hartree-Fock (HF) technique for the electronic part, totally unrestricted in both spin *and* direct space [9–12] — for our problems, this is superior to traditional homogeneous HF approaches — and a classical treatment for the lattice part. To the generally inhomogeneous HF configurations, we have added a similarly inhomogeneous RPA analysis of linear fluctuations to calculate infrared (IR) active phonon modes shown here and other dynamical properties to be reported elsewhere.

The general model Hamiltonian we consider is

$$H = \sum_{i\neq j,\sigma} t_{ij}(\{u_k\})c^\dagger_{i\sigma}c_{j\sigma} + \sum_{i,\sigma} e_i(\{u_k\})c^\dagger_{i\sigma}c_{i\sigma} + \sum_i U_i c^\dagger_{i\uparrow}c^\dagger_{i\downarrow}c_{i\downarrow}c_{i\uparrow} + \sum_{\langle i\neq j\rangle,\sigma,\sigma'} U_{ij}c^\dagger_{i\sigma}c^\dagger_{j\sigma'}c_{j\sigma'}c_{i\sigma} + \sum_l \frac{1}{2M_l}p_l^2 + \sum_{k,l}\frac{1}{2}K_{kl}u_k u_l. \quad (1)$$

Here, $c^\dagger_{i\sigma}$ creates a *hole* with spin σ at site i in the Cu $d_{x^2-y^2}$ or the O $p_{x,y}$ orbital. For the lattice part, we study only the motion of O ions along the Cu-O bonds and assume that only diagonal components of the spring-constant matrix are finite, $K_{kl} = \delta_{k,l}K$, for simplicity. For electron-lattice coupling, we assume that the nearest-neighbor Cu-O hopping is modified by the O-ion displacement u_k as $t_{ij} = t_{pd} \pm \alpha u_k$, where the + (−) applies if the bond shrinks (stretches) with positive u_k. The Cu-site energy is assumed to be modulated by the O-ion displacements u_k linearly as $e_i = \epsilon_d + \beta\sum_k(\pm u_k)$, where the sum extends over the four surrounding O ions; here the sign takes + (−) if the bond becomes longer (shorter) with positive u_k. The other electronic matrix elements are O-O hopping ($-t_{pp}$) for t_{ij}, O-site energy (ϵ_p) for e_i, with $\Delta = \epsilon_p - \epsilon_d$, Cu-site ($U_d$) and O-site ($U_p$) repulsions for U_i, and the nearest-neighbor Cu-O repulsion (U_{pd}) for U_{ij}. Parameter values are used in regimes relevant to the copper oxides. We have taken $t_{pd} = 1$, $t_{pp} = 0.5$, $\Delta = 3$, $U_d = 8$, $U_p = 3$, and $U_{pd} = 1$. (This parameter set is taken from constrained LDA calculations [5].) The above-defined parameters and $\lambda_\alpha = \lambda_\beta = 0$ are hereafter termed the reference parameter set: $\lambda_\alpha = \alpha^2/(Kt_{pd})$, $\lambda_\beta = \beta^2/(Kt_{pd})$. We vary λ_α, λ_β, U_{pd}, and U_d. We change Δ with U_{pd} and U_d so as to maintain a constant renormalized energy difference between Cu and O levels in the undoped case. Comparison of our results for local lattice distortion and reduced Cu magnetic moments accompanied by added holes with generalized, inhomogeneous LDA calculations [13] is consistent, e.g., with val-

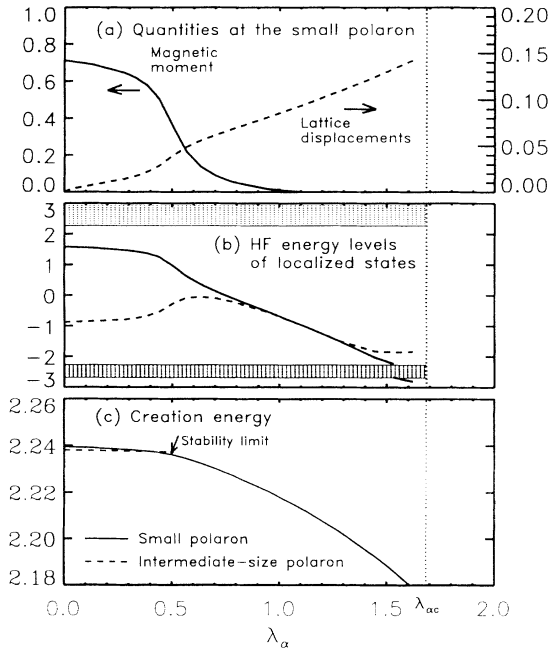

FIG. 1. (a) Magnetic moment on the central Cu site of the small polaron and ratio of lattice displacement of the surrounding O to Cu-O distance (1.89 Å), (b) gap energy levels, and (c) creation energy $\epsilon_1 = E^{N+1} - E^N - \bar{\mu}$, for the small polaron state as a function of λ_α. Other energy levels in the gap close to the bands (shaded areas) are not shown. E^{N+i} is the total energy with i added holes and $\bar{\mu}$ is the midgap energy. We also show in (c) ϵ_1 for the intermediate-size ferromagnetic polaron. All energies are in units of t_{pd}. Parameters are $t_{pd} = 1$, $t_{pp} = 0.5$, $\Delta = 4$, $U_d = 10$, $U_p = 3$, $U_{pd} = 1$, and $K = 32t_{pd}/\text{Å}^2$. The dotted line at $\lambda_{\alpha c} \simeq 1.68$ marks the stability limit of the AF ground state at stoichiometry.

ues of $\lambda_\alpha = 0.28$, $\lambda_\beta = 0$, and $K = 32t_{pd}/\text{Å}^2$. The effect of other kinds of electron-lattice coupling, like motion of the Cu ions or apical O [14], will be reported elsewhere.

Mean-field states were obtained by solving the unrestricted HF Hamiltonian with self-consistency conditions for on-site and nearest-neighbor charge and spin densities, as well as lattice displacements, without assumption on the form of these quantities [9–12]. The self-consistency equations are obtained by minimizing the total energy with respect to these quantities which are treated as classical numbers. The kinetic part of the lattice is incorporated with particle-hole excitations into the RPA analysis below. We have not investigated restoration of translational symmetry. This is necessary for polaron band formation and transport but is beyond the present scope of the RPA. Calculations were made on systems of 6×6 CuO_2 unit cells with periodic boundary conditions.

In the reference parameter set, each added hole is localized primarily on a single Cu site and four surrounding O sites. The spin density at the central Cu site is in the opposite direction to the undoped case, so that it is termed a small ferromagnetic polaron. The spin densi-

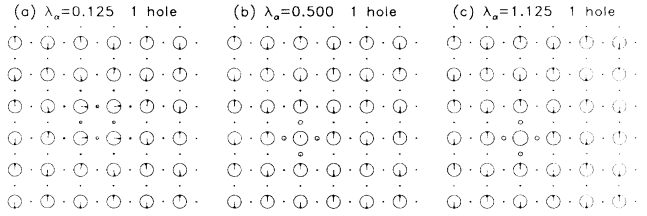

FIG. 2. Charge (radii of the circles) and spin (arrows) densities (see Refs. [9,11] for definitions) in the one-hole doped systems, (a) with the intermediate-size polaron; and (b),(c) with the small polaron. The arrows are normalized so as to touch the circle if completely polarized. Big (small) circles are Cu (O). Parameters are as in Fig. 1.

ties at the four O sites are small and have the opposite direction to that at the central Cu site. As λ_α is turned on, the Cu magnetic moment is reduced and the O ions displace toward the central Cu. Similar structures are also found for $U_d = 10$, $\Delta = 4$ [see Figs. 2(b) and 2(c)]. For these structures, five HF eigenstates appear inside the charge-transfer gap per added hole. These states are occupied by holes and their associated HF wave functions are spatially localized. Among the five, two are located deep inside the gap [Fig. 1(b)] and are well localized: The higher one corresponds to an oxygen state formed by the four O that surround a Cu and has smaller weight on the Cu. The lower one corresponds mainly to the central Cu, has opposite spin to the previous one, and has smaller weight on the four O. In a Zhang-Rice picture this many-body state mixes with a similar state in which the directions of the spins on the Cu and the O are reversed. Because such a correlated state cannot be constructed with a single Slater determinant, HF fails to describe it properly. However, we expect much of the energetics of the state to be captured at the unrestricted mean-field level.

Once the added hole is localized around a Cu with a reversed spin, a very interesting feedback mechanism is set up between the $\uparrow$ and $\downarrow$ spin levels of the central Cu at energies $\sim \epsilon_d$ and $\sim \epsilon_d + U_d$, and the $\uparrow$ and $\downarrow$ O levels at $\sim \epsilon_p$ corresponding to the symmetric combination of the four O orbitals. (We neglect here the effect of U_p for simplicity.) The $\downarrow$ level on the O mixes with the unoccupied $\downarrow$ level at $\sim \epsilon_d + U_d$. This means that some non-negligible amount of double occupancy is generated on the central Cu. As a consequence the Cu $\uparrow$ level, initially at ϵ_d, is pushed up from the lower Hubbard band. The lower level in the gap [dashed line in Fig. 1(b)] results from the mixing of this level and the O $\uparrow$ level. The higher the Cu $\uparrow$ level moves, the bigger the mixing. This reduces the amount of charge in the Cu $\uparrow$ orbital pulling down the state originally at $\epsilon_d + U_d$. The upper level in the gap results from the mixing of this state with the O $\downarrow$ level [solid line in Fig. 1(b)]. Clearly this process feeds back positively: The $\downarrow$ level on the O mixes more and more with the $\downarrow$ level on the Cu, generating even more double occupancy and the two levels on the Cu approach each

other as do the two levels in the gap.

The interplay with the lattice is also important. The strong mixing of the four surrounding O with the central Cu allows the state to gain energy if the O approach ($\lambda_\alpha \neq 0$) the Cu. This locally increases the covalency between Cu and O and the above mechanism is strongly amplified: covalency and the displacements of the O ions reinforce each other synergistically. The result is that for a moderate value of the electron-lattice coupling strength λ_α relative to the $\lambda_{\alpha c}$ defined below, both $\uparrow$ and $\downarrow$ level on the Cu become nearly degenerate and the magnetic moment on the central Cu collapses [see Fig. 1(a)]. One can visualize this quenching with λ_α as a rapid crossover from a Heitler-London-like state corresponding to the Zhang-Rice singlet to a highly covalent molecular state. If the system is doped with an electron a small polaron is also formed: an interesting feature of these states is that the large shifts in the single-particle energy levels toward the center of the gap result in them lying similarly for both the hole- and electron-doped cases, as found in spectroscopic experiments [15].

If λ_α is increased even more, covalency is locally enhanced and correspondingly the two levels in the gap go down. Finally they approach the lower Hubbard band and one crosses it, whereas the other with opposite symmetry (spin flip) gets repelled by the band states. Above a critical value $\lambda_{\alpha c}$ the *undoped* ground state is replaced by a nonmagnetic bond-order-wave state. Interesting local doping states are found in this regime involving spin and charge separation, as will be shown elsewhere. Note that the strong local effects of intersite electron-lattice coupling upon doping occur in a regime extending significantly below $\lambda_{\alpha c}$ [see Figs. 1(a) and 1(b)].

If the parameters (U_d, Δ) are increased simultaneously from the LDA values to the values (10,4), a new state appears for small λ_α. The state is an intermediate-size ferromagnetic polaron [see Fig. 2(a)]. It extends to about four Cu sites and their surrounding O sites, and if $\lambda_\alpha < 0.4$ its energy is lower than the small polaron energy [see Fig. 1(c)]. When (U_d, Δ)=(8,3) the former becomes unstable. The spin densities at these Cu sites are almost in the same direction and perpendicular to the background AF Cu spins. Inside the polaron, the spin densities at the O sites are small. Around the polaron, the Cu spin densities have small ferromagnetic components decaying slowly with distance. Correspondingly, the HF eigenstates inside the charge-transfer gap appear closer to the bands, reflecting a more extended texture than the small polaron. We can anticipate tunneling between the small and intermediate-size polarons when full quantum fluctuations are included.

The effect of finite λ_β is very weak up to a certain critical value ($\lambda_{\beta c} \simeq 1.2$) at which the ground state changes to a charge-density-wave state. In contrast to Fig. 1 the Cu magnetic moment remains almost constant for $\lambda_\beta < \lambda_{\beta c}$. When (U_d, Δ) is decreased from (10,4) to (8,3) the $\lambda_{\alpha c}$, $\lambda_{\beta c}$, and the crossover λ_α are rescaled towards lower values by a ratio of 8/10 showing that U_d fixes the energy scale for $\lambda_{\alpha c}$.

Large values of U_{pd} produce phase separation as found in other approaches [6]. Details will be given elsewhere.

As seen above, doping states are very sensitive to small changes of the parameters in the Hamiltonian and a purely analytical determination of the true ground state is very difficult. On the other hand, an experimental distinction between them is possible through their differing spectroscopic signatures. In Fig. 3 we show IR absorption spectra obtained from the current-current correlation functions. Raman spectra and electronic optical absorption spectra will be described elsewhere. To evaluate the IR absorption spectra, we used the adiabatic approximation in the RPA [16,17], where quadratic and higher-order terms with respect to frequency are neglected in the RPA electronic bubble. In the phonon-frequency range, including the IR range, this approximation is expected to work well, as is supported by comparison with nonadiabatic inhomogeneous RPA results [11,12] on small systems. With $K = 32 t_{pd}/\text{Å}^2$, bare phonons ($\lambda_\alpha = \lambda_\beta = 0$) oscillate with $\omega = 0.0914$. For $t_{pd} = 1.3$ eV this corresponds to 840 cm^{-1} which is comparable with the in-plane stretching IR active mode found in La_2CuO_4 (706 cm^{-1}) [8]. As the electron-lattice coupling λ_α increases, phonons are further softened. In the state with an intermediate-size ferromagnetic polaron [Fig. 2(a)], IR active phonon modes are induced at $\omega = 0.0768$ and $\omega = 0.0875$ [Fig. 3(a)], which correspond to "shape oscillations" of the intermediate-size ferromagnetic polaron.

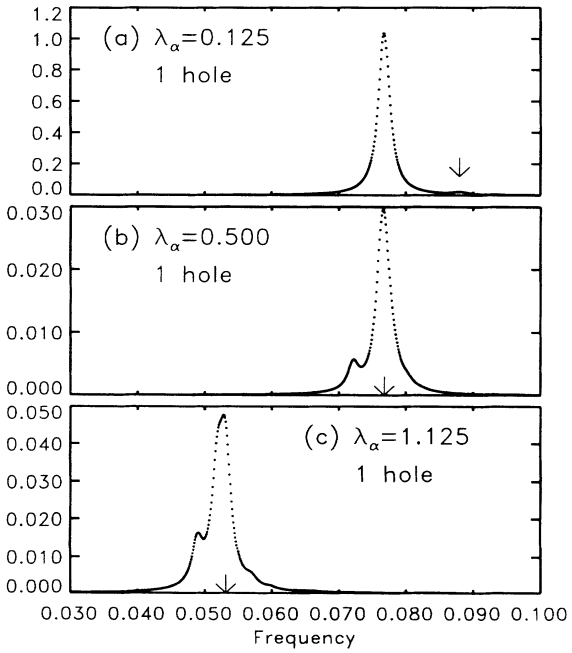

FIG. 3. Infrared absorption spectra in the one-hole doped systems, (a) with the intermediate-size polaron; and (b),(c) with the small polaron. Arrows indicate the positions of the undoped infrared peaks. Same parameters as in Fig. 1.

Namely, the two O ions on the horizontal Cu-O-Cu bonds inside the polaron move in the same direction as do those on the vertical Cu-O-Cu bonds. Soft electronic modes mix with the phonon modes giving a very large oscillator strength for the doping peak (at $\omega = 0.0768$) as compared with the undoped peak at $\omega = 0.0880$.

In the states with a small polaron [Figs. 2(b) and 2(c)], local IR active phonon modes appear at $\omega = 0.0722$ [2(b)]; and $\omega = 0.0489, 0.0519$ [2(c)], which produce structure on the low-energy side of the undoped main peak [Figs. 3(b) and 3(c)]. These modes correspond to antisymmetric oscillations of pairs of opposite O ions with respect to the central Cu of the small polaron. These IR spectra are consistent with the experimentally observed [8] bleaching of phonon modes and intensity shift to lower frequencies. Because we are not including all the relevant phonons we postpone a detailed comparison. Also observed in the same experiments [8] is a bleaching of the interband electronic absorption and the corresponding activation of an electronic absorption in the gap, which we can qualitatively associate with the appearance of gap states [Fig. 1(b)]. Correlation of these high-energy features with low-energy structure corresponding to particular phonons through Raman excitation profiles is under way. *Electron*-doped cases will also be reported elsewhere. Interestingly the IR local modes lie above the stoichiometric IR frequency in these cases.

In conclusion, we have used a convenient inhomogeneous HF plus RPA approach to study hole doping states in the 2D, three-band Peierls-Hubbard model. We find that the competition of broken-symmetry ground states in this model is extremely sensitive to parameter values. Nonlinear feedback effects produce a rapid crossover from a Zhang-Rice regime to a molecular singlet state with local quenching of the Cu moment and large local lattice distortion, induced by intersite-electron-lattice coupling strengths in a regime extending substantially below the critical value for destruction of the AF state in the undoped system. Other possible states, including intermediate-size ferromagnetic polarons and phase separation, were also identified. Possible hole pairing tendencies remain to be studied. However, we emphasize here that the various doping states are characterized by distinct high-energy (electronic optical absorption) and low-energy (IR, Raman) signatures relevant to chemical-doping and photodoping experiments [7, 8].

[1] P. W. Anderson, Science **235**, 1196 (1987).

[2] V. J. Emery, Phys. Rev. Lett. **58**, 2794 (1987); J. E. Hirsch, Phys. Rev. Lett. **59**, 228 (1987); C. M. Varma, S. Schmitt-Rink, and E. Abrahams, Solid State Commun. **62**, 681 (1987); Z. Tešanović, A. R. Bishop, and R. L. Martin, Solid State Commun. **68**, 337 (1988).

[3] Different magnetic polarons have also been discussed recently from other starting points than assumed in this work; e.g., D. Emin and M. S. Hillery, Phys. Rev. B **37**, 4060 (1988).

[4] F. C. Zhang and T. M. Rice, Phys. Rev. B **37**, 3759 (1988).

[5] M. S. Hybertsen, M. Schlüter, and N. E. Christensen, Phys. Rev. B **39**, 9028 (1989).

[6] J. E. Hirsch, E. Loh, Jr., D. J. Scalapino, and S. Tang, Phys. Rev. B **39**, 243 (1989); S. A. Trugman, Phys. Scr. **T27**, 113 (1989); J. Lorenzana and L. Yu, Mod. Phys. Lett. B **5**, 1515 (1991); M. Grilli, R. Raimondi, C. Castellani, C. Di Castro, and G. Kotliar, Phys. Rev. Lett. **67**, 259 (1991).

[7] G. A. Thomas, D. H. Rapkine, S. L. Cooper, S-W. Cheong, and A. S. Cooper, Phys. Rev. Lett. **67**, 2906 (1991); G. A. Thomas, D. H. Rapkine, S-W. Cheong, and L. F. Schneemeyer (unpublished).

[8] Y. H. Kim, S-W. Cheong, and Z. Fisk, Phys. Rev. Lett. **67**, 2227 (1991); G. Yu, C. H. Lee, A. J. Heeger, N. Herron, and E. M. McCarron, Phys. Rev. Lett. **67**, 2581 (1991); C. Taliani, A. J. Pal, G. Ruani, R. Zamboni, X. Wei, and Z. V. Vardeny, in *Electronic Properties of High-T_c Superconductors and Related Compounds*, edited by H. Kuzmany, M. Mehring, and J. Fink (Springer-Verlag, Berlin, Heidelberg, 1990), and references therein.

[9] For recent studies, see, for example, A. Singh and Z. Tešanović, Phys. Rev. B **41**, 614 (1990); J. A. Vergés, E. Louis, P. S. Lomdahl, F. Guinea, and A. R. Bishop, Phys. Rev. B **43**, 6099 (1991); M. Inui and P. B. Littlewood, Phys. Rev. B **44**, 4415 (1991).

[10] J. Zaanen and O. Gunnarsson, Phys. Rev. B **40**, 7391 (1989).

[11] K. Yonemitsu, I. Batistić, and A. R. Bishop, Phys. Rev. B **44**, 2652 (1991).

[12] K. Yonemitsu and A. R. Bishop, Phys. Rev. B **45**, 5530 (1992).

[13] V. I. Anisimov, M. A. Korotin, J. Zaanen, and O. K. Andersen, Phys. Rev. Lett. **68**, 345 (1992).

[14] I. Batistić, A. R. Bishop, R. L. Martin, and Z. Tešanović, Phys. Rev. B **40**, 6896 (1989).

[15] J. W. Allen *et al.*, Phys. Rev. Lett. **64**, 595 (1990).

[16] I. Batistić and A. R. Bishop, Phys. Rev. B **45**, 5282 (1992).

[17] H. Ito and Y. Ono, J. Phys. Soc. Jpn. **54**, 1194 (1985); A. Terai, Y. Ono, and Y. Wada, J. Phys. Soc. Jpn. **55**, 2889 (1986); K. Yonemitsu, Y. Ono, and Y. Wada, J. Phys. Soc. Jpn. **56**, 4400 (1987).